Coupled poro-elasto-plastic models of transient fluid flow in response to a crustal strike-slip fault: insight from a geothermal setting in the South Andean Volcanic Zone

Sáez-Leiva F., Gerbault M., Ruz-Ginouves J., Iturrieta P., Hurtado D.E., Cembrano J.

1. Aim & Motivation

Geothermal systems can host energy resources, where hydrothermally enhanced chemical reactions can favour mineralizations of economic interest. While faults can alter fluid flow in their surroundings, potentially acting as barriers or conduits for fluids, magmatic and hydrothermal fluids can also modify pore pressure and alter faults resistance to slip motion. The Planchón-Peteroa geothermal system, located in the South Andean Volcanic Zone (Chile), illustrates how crustal scale strike-slip faults are associated with localized hydrothermal fluid flow. In this work, we address the first-order, time-dependent control a strike-slip crustal fault exerts on a nearby geothermal system, using the Planchón-Peteroa geothermal system as a case study.

How?

We developed an original poro-elasto-plastic Finite Element Method (FEM) model based on the FEniCS library, in which the poro-elastic and the elasto-plastic constitutive equations are implicitly coupled. Once this implementation is benchmarked, we assess the development of fluid flow due to a left-lateral fault slip set at 5 km depth considering the influence of the fault's slip-rate, shear modulus and permeability, the plastic yield strength, and the fluid's viscosity.

The Suction Pump Mechanism (Sibson 1985, 1987, 2000)

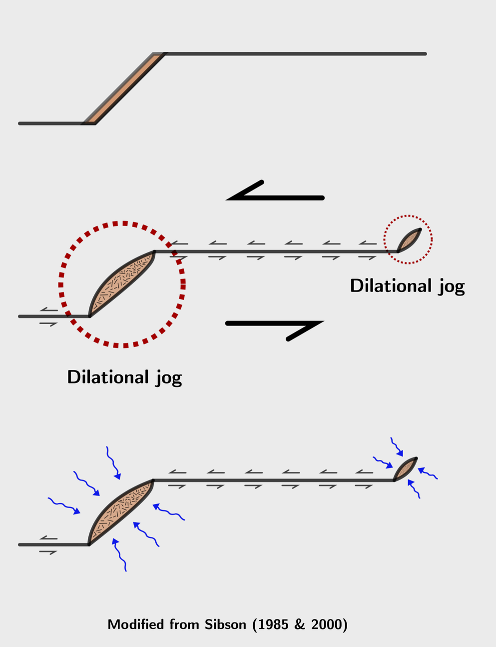

Refers to fluid migration towards a slipping strike-slip fault system because of the emergence of dilational jogs, from pre-existing stepovers on the trace of the fault. These jogs experience a sudden dilation, causing a fluid pressure drop inducing suction on the surrounding fluid.

2. The Planchón-Peteroa geothermal system

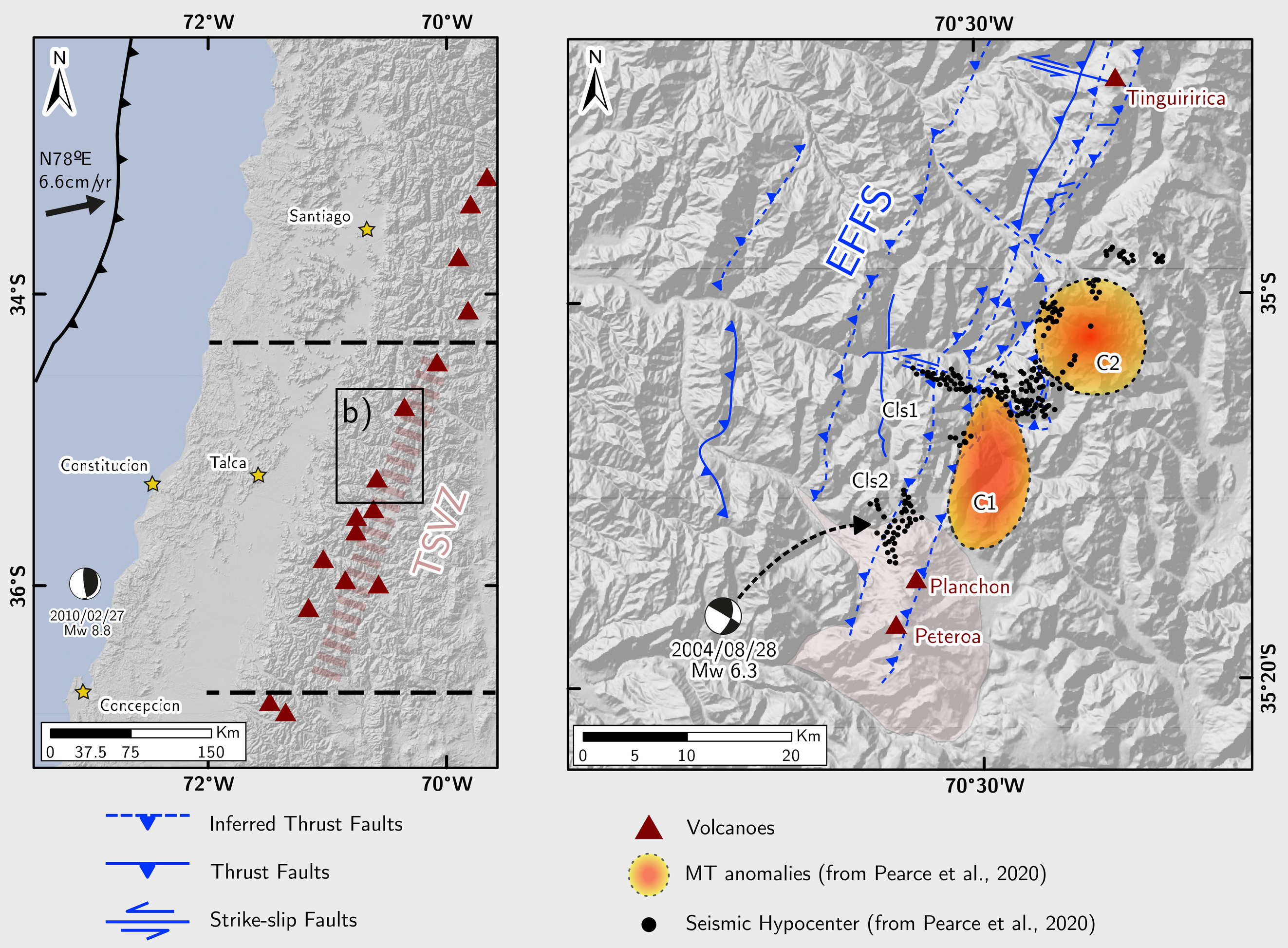

Even though further local studies are yet to be conducted, the Planchón-Peteroa inferred geothermal system displays the fundamental traits of an Andean high-enthalpy geothermal system:

- WNW-striking seismogenic faults
- Highly conductive rock volumes in between and close to these faults
- Hotsprings

Magnetotelluric and seismic surveys in the region have constrained the geometry and location of these regional fault systems and the inferred fluid reservoirs and have determined that fluids are closely related to rock deformation (Pearce et al., 2020).
We focus on the influence of the seismically active WNW-striking, left lateral Andean Transverse Fault (ATF) (seismic cluster Cls1) on the geothermal reservoir located NE of the Planchón volcano at 4-8 km depth, inferred from the C1 resistive anomaly.

3. Numerical approach: a FEniCS-based poro-elasto-plastic model

Equations

- Mass balance

$$\alpha \frac{\partial \varepsilon_v(\boldsymbol{u})}{\partial t} + \frac{1}{M}\frac{\partial \mathrm{p}}{\partial t} + \mathrm{div}\left(\boldsymbol{q}(\mathrm{p})\right) = 0$$

$$\boldsymbol{q}(\mathrm{p}) = -\frac{\kappa}{\mu}\nabla \mathrm{p}$$

- Linear momentum balance

$$\mathrm{div}\left(\boldsymbol{\sigma}(\boldsymbol{u}, \mathbf{p})\right) = 0$$

$$\boldsymbol{\sigma}(\boldsymbol{u}, \mathrm{p}) = \left(K - \frac{2G}{3}\right)\mathrm{trace}\left(\boldsymbol{\varepsilon}(\boldsymbol{u})\right)\boldsymbol{I} + 2G\boldsymbol{\varepsilon}(\boldsymbol{u}) - \alpha \mathrm{p}$$

- Elastoplasticity

$$\boldsymbol{\varepsilon} = \boldsymbol{\varepsilon}^e + \boldsymbol{\varepsilon}^p$$

$$\Delta\boldsymbol{\sigma} = \boldsymbol{D} : \Delta\boldsymbol{\varepsilon}^e + \boldsymbol{D}^{plas} : \Delta\boldsymbol{\varepsilon}^p$$

$$f(\boldsymbol{\sigma}, \bar{\varepsilon}^p) = \sqrt{3J_2(\boldsymbol{s}(\boldsymbol{\sigma}))} - \left(\sigma_{y0} + H\bar{\varepsilon}^p\right) \leq 0$$

*We solve for the fluid pressure **p** and the solid displacement **u***

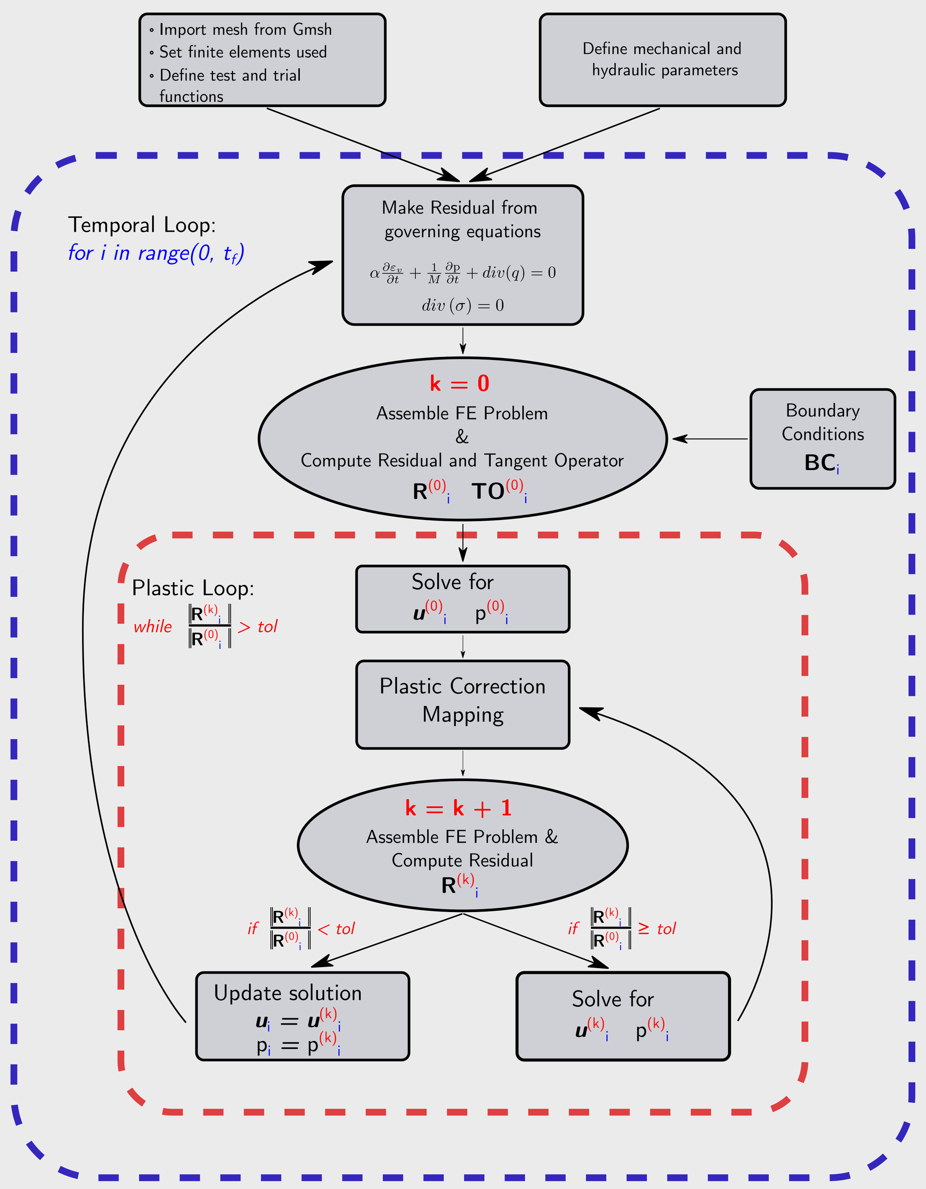

The poro-elasto-plastic formulation is numerically solved using a Finite-Element scheme implemented in the Python opensource library FEniCS: a collaborative effort to solve complex differential equations (Alnæs et al., 2015). We use the latest legacy version (2019.1.0) of FEniCS which documents previous poromechanical studies (e.g. Haagensen et al., 2020).

Our benchmarks

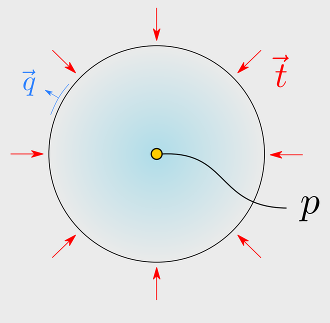

Cryer's Problem (Cryer, 1963)

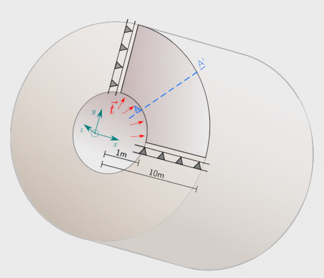

Thick-walled elasto-plastic cylinder (Nadai, 1950)

Results available at our GitHub!
https://github.com/FNSL1996/PEP_FEniCS

4. Results: Solid deformation and fluid flow evolution

Our model

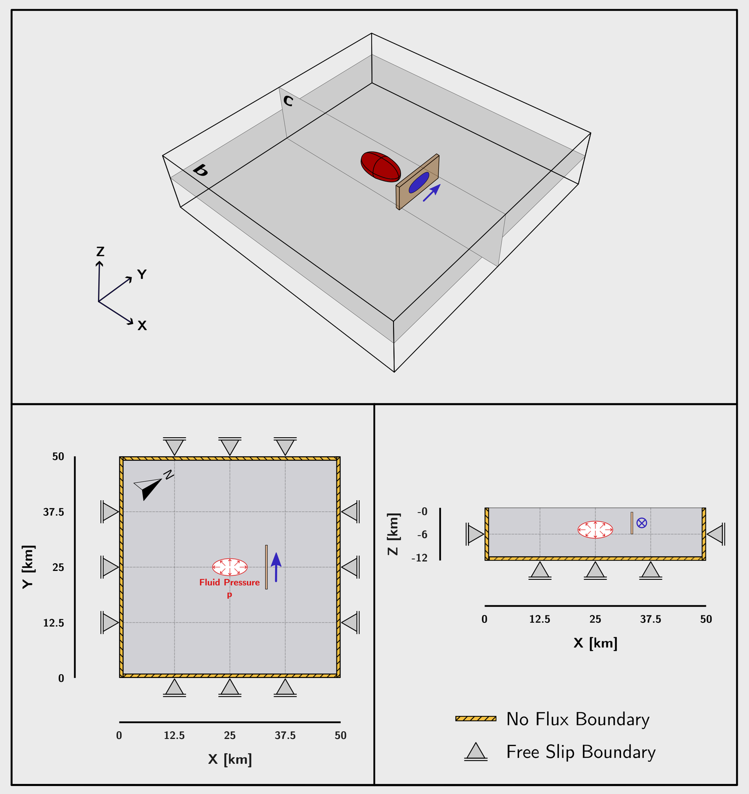

We use a Berea Sandstone for our reference model

G [GPa]	ν [-]	K [GPa]	K_s [GPa]	K_f [GPa]	α [-]	ϕ [-]	κ [m^2]	M [GPa]
6	0.2	8	36	2.25	0.778	0.19	$1.90\cdot10^{-13}$	9.92

Reference Model: Solid Behavior

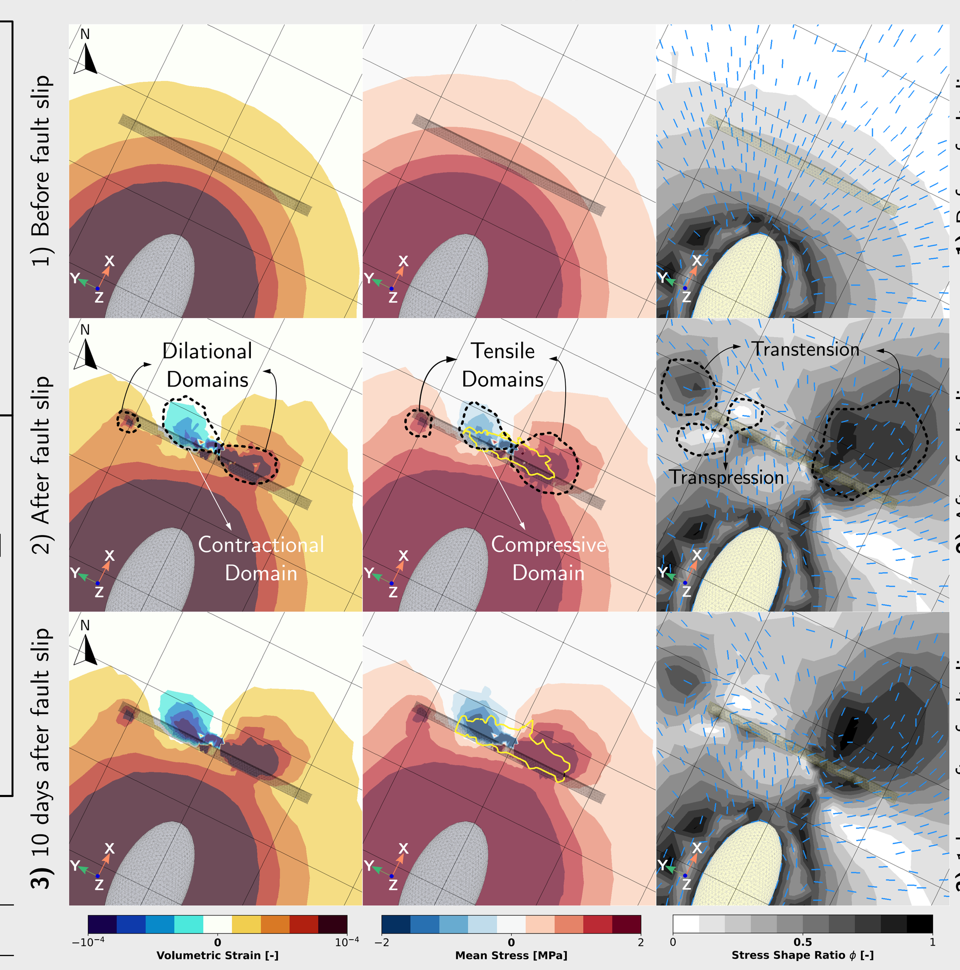

Reference Model: Fluid flow evolution

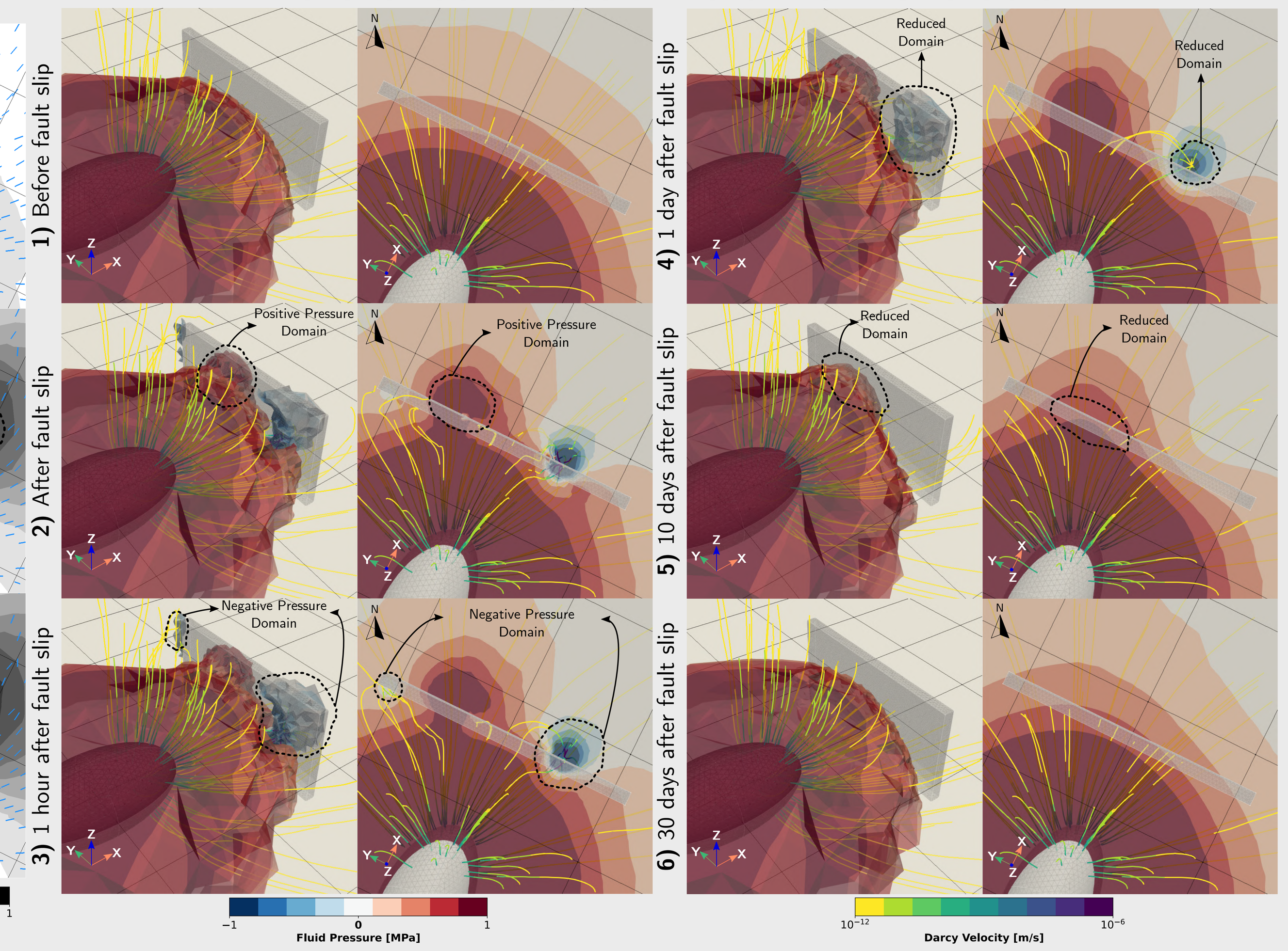

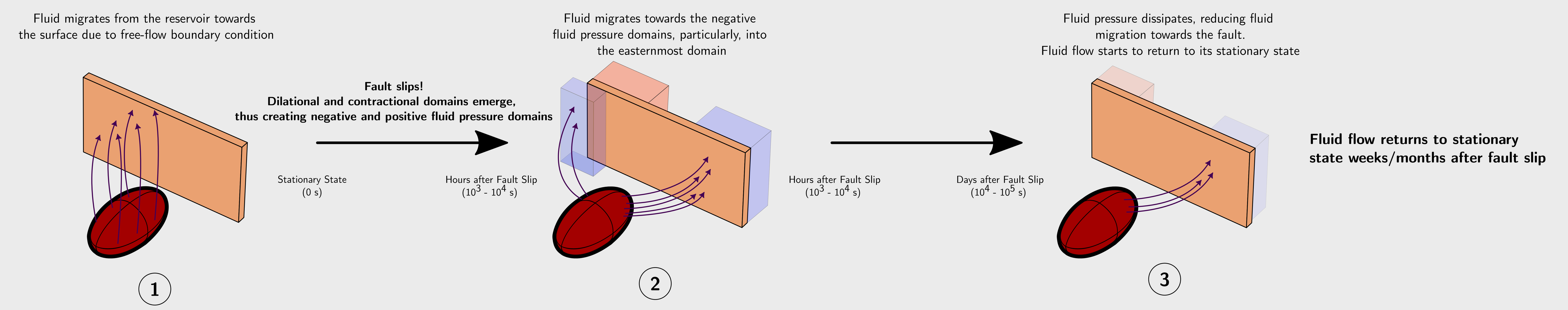

5. Results: Fluid flux variation over time

Model Name	Rheology and Heterogeneity	Slip-rate [m/s]	G_f [GPa]	κ_f [m^2]	σ_{y0} [MPa]	μ [Pa · s]	NF^{MAX} [-]
Elastic_SR_1	**P-Elastic**, Homogeneous	**0.1**	6	$1.90\cdot10^{-13}$	*	10^{-3}	~10
SR_01	P-EPlas, Homogeneous	**0.1**	6	$1.90\cdot10^{-13}$	5	10^{-3}	~10
SR_1	P-EPlas, Homogeneous	1	6	$1.90\cdot10^{-13}$	5	10^{-3}	~12
SR_10	P-EPlas, Homogeneous	**10**	6	$1.90\cdot10^{-13}$	5	10^{-3}	~12
Yield_SR_1	P-EPlas, Homogeneous	1	6	$1.90\cdot10^{-13}$	**2**	10^{-3}	~11
Shear_SR_1	P-EPlas, **Compliant Fault**	1	**3**	$1.90\cdot10^{-13}$	5	10^{-3}	~8
Permeability_SR_1	P-EPlas, **Permeable Fault**	1	6	$\mathbf{4.86\cdot10^{-10}}$	5	10^{-3}	~15
Viscosity_SR_1	P-EPlas, Homogeneous	1	6	$1.90\cdot10^{-13}$	5	$\mathbf{10^{-2}}$	~75

Area used for flux calculation

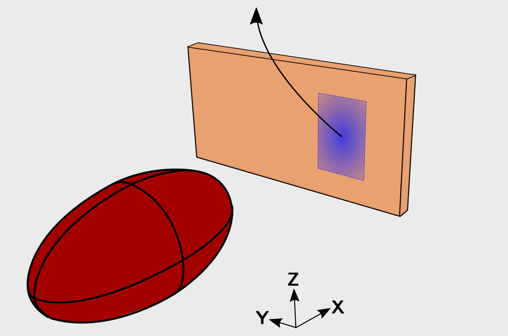

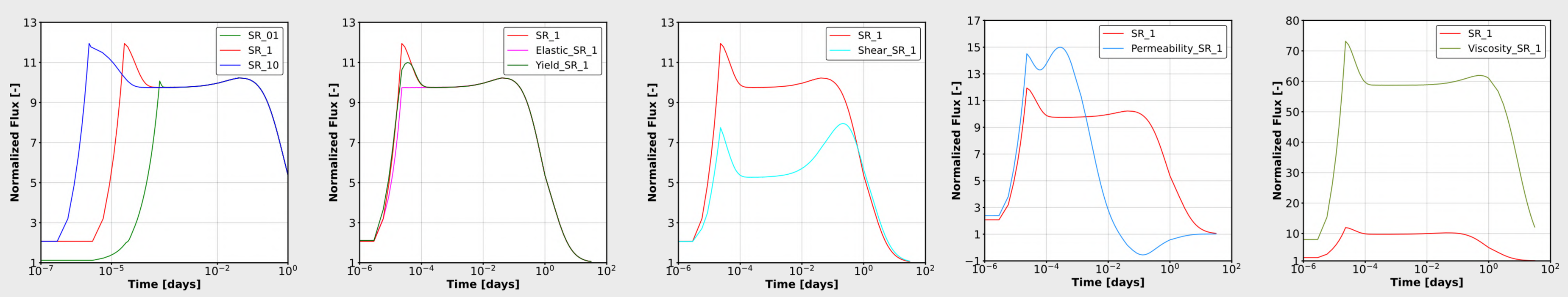

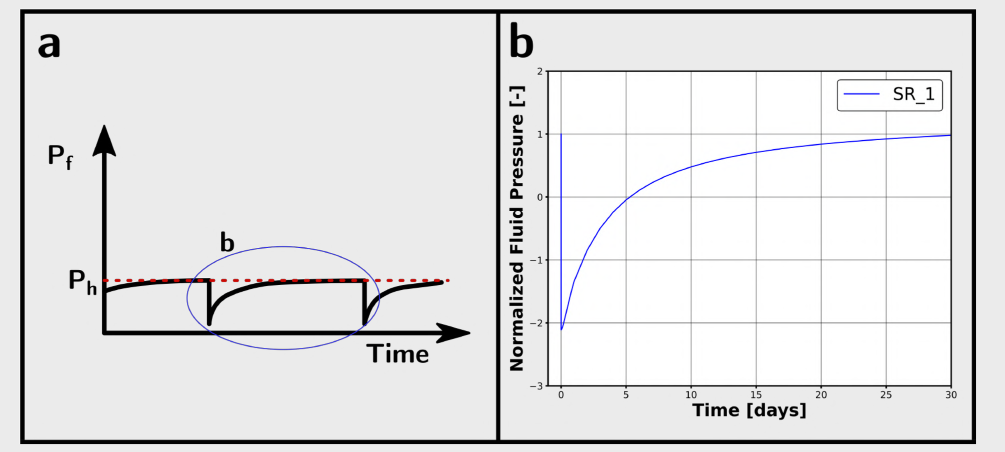

a) Suction pump mechanism at a dilational jog (Sibson, 2000), with coseismic reduction in fluid pressure (Pf) below hydrostatic pressure (Ph), and progressive increase back to Ph in the interseismic period.
b) Normalised fluid pressure at the eastern negative pressure domain in our models. A rapid decrease in fluid pressure is seen during fault slip, followed by a progressive return to stationary level 30 days afterfault slip, remarkably similar to (a).

Stages of fluid flux evolution

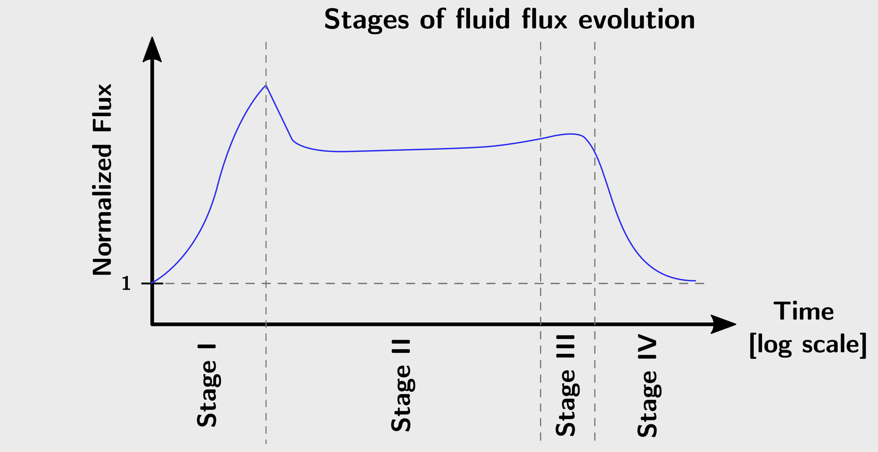

6. Conclusion

We postulate that the first-order control over fluid flow for fault and geothermal system as the ones present in the South Andean Volcanic Zone is that of a suction pump-like mechanism. Our results show a time-dependent focussed fluid flow, which can alter the stationary fluid flow from weeks to months.

- The spatial and temporal evolution of this fluid flow is shown to depend on fault permeability (greater oscillation range), shear modulus (lower flow), fluid viscosity and on the rock's yield strength (greater flow).
- We report a maximum fluid flux reaching 8 to 70 times the initial stationary flux.
- We also show how the simple von Mises plasticity criterion already enhances fluid flow, locally.

Read our work!

Our paper

Our GitHub Repository

References:

Alnæs M, Blechta, Hake, et al., 2015. The Fenics project version 1.5. Arch.Num. Softw. 3-100, 9-23
Cryer, C.W., 1963. A comparison of the three-dimensional consolidation theories of Biot and Terzaghi. Q. J. Mech. Appl. Math. 16, 401–412
Gerbault, M., Poliakov, A.N., Daignieres, M., 1998. Prediction of faulting from the theories of elasticity and plasticity: what are the limits? J. Struct. Geol. 20, 301–320.
Haagenson, R., Rajaram, Allen, 2020. A generalized poroelastic model using Fenics,... Comput. Geosci.
Nadai, A., 1950. Theory of Flow and Fracture of Solid. McGraw-Hill, New York.
Sibson, R.H., 1985. Stopping of earthquake ruptures at dilational fault jogs. Nature 316 (6025), 248–251
Sibson, R.H., 1987. Earthquakes rupturing as a mineralizing agent in hydrothermal systems. Geology 15 (8).
Sibson, R.H., 1990. Conditions for fault-valve behaviour. Geol. Soc.Spec.Pub. 54 (1), 15–28
Sibson, R.H., 2000. Fluid involvement in normal faulting. J. Geodyn. 29 (3–5), 469–499.
...and many more!